

Al molar ratio of 2:1 was titrated with 0.1 M NaOH solution to approximately pH 9.5 under an N<sub>2</sub> atmosphere and aged for 24 h with vigorous stirring. The resulting white precipitate was collected by centrifugation and washed thoroughly with decarbonated water. The DNA-LDH hybrid was then prepared by intercalating double-stranded DNA into the interlayer space of the pristine LDH by an anion-exchange route. The DNA solution (2.6 mg mL<sup>-1</sup>) was added to the LDH suspension (1 mg mL<sup>-1</sup>) and mixed together in a shaking incubator for 7 days at 65 °C. The resulting DNA-LDH hybrid was collected by centrifugation and washed with decarbonated water. For the preparation of PEO-coated DNA-LDH hybrid, 0.05 g of the DNA-LDH hybrid was dispersed in 50 mL of EtOH, and 50 mL of 0.5 % PEO-EtOH solution was added. After 30 min the PEO-coated DNA-LDH hybrid was washed with EtOH and then dried.

**Preparation of PPY-MAG Hybrid:** The MAG (maghemite) nanoparticles were prepared by the method of Massart et al. [15,16]. FeCl<sub>3</sub>·6H<sub>2</sub>O (44.74 g) and FeCl<sub>2</sub>·4H<sub>2</sub>O (16.45 g) with an Fe<sup>2+</sup>/Fe<sup>3+</sup> ratio of 0.5 were dissolved in deionized water, and heated to 50 °C. Then, 150 mL of 8.6 M NH<sub>4</sub>OH solution was quickly added to the solution with vigorous mechanical stirring. The precipitated magnetite (Fe<sub>3</sub>O<sub>4</sub>) was washed with deionized water and acetone, and magnetically decanted to remove the chloride ions and other non-magnetic impurities. The obtained magnetite was easily oxidized to maghemite as follows [13,17]. The magnetite (18 g) was treated with 2 M nitric acid solution for 15 min and 300 mL of aqueous 0.33 M iron(III) nitrate solution was then added. The resulting mixture was then boiled for another 15 min. The resulting maghemite particles were washed and dried in vacuo for subsequent polypyrrole coating. 1.7 g of maghemite was dispersed in liquid pyrrole for 30 min, and excess pyrrole was removed by magnetic decantation. This maghemite/pyrrole mixture was added to 200 mL of 0.15 M FeCl<sub>3</sub>/EtOH solution with stirring for 30 min to polymerize the surface pyrrole. Finally, the PPY/γ-Fe<sub>2</sub>O<sub>3</sub> nanohybrids were washed with ethanol, separated by magnetic decantation, and dried in vacuo.

**DNA Stability Test under Enzyme Conditions:** 96 units of DNase I (purchased from Sigma) was added to the DNA-LDH hybrid (15 μg) mixed with Ca<sup>2+</sup>/Mg<sup>2+</sup> ions and incubated at 37 °C. After 2 h, the activation of DNase I was stopped by heating to 75 °C for 30 min. The hybrid was then washed with decarbonated water. For the recovery of DNA from the hybrid, both the as-prepared DNA-LDH hybrid and the DNase I treated sample were acidified to a pH of about 2 with 0.01 M HCl solution for 30 min. The extracted DNA strands were amplified by PCR. Typical PCR was performed in 25 μL PCR buffer containing 200 μM of dNTPs (deoxynucleoside triphosphates), 0.2 μM of forward primer (AGGGT CGAAG TACGG AATAC), 0.2 μM of reverse primer (GTCCG GAGCA CTCCG CTCCG) and 1 U of Taq polymerase (Nova-taq, Genemed). Thermocycling was at 95 °C for 10 min followed by 35 cycles of 95 °C for 30 s, 60 °C for 30 s, 72 °C for 30 s, and then 72 °C for 10 min.

Received: January 9, 2004  
Final version: March 29, 2004

[1] M. Blaxter, *Nature* **2003**, 421, 122.  
[2] C. T. Clelland, V. Risca, B. Carter, *Nature* **1999**, 399, 533.  
[3] J. P. L. Cox, *Trends Biotechnol.* **2002**, 19, 247.  
[4] J. P. L. Cox, *Analyst (London)* **2001**, 126, 545.  
[5] N. Winssinger, J. L. Harris, B. J. Backes, P. G. Schultz, *Angew. Chem. Int. Ed.* **2001**, 40, 3152.  
[6] J. Nam, C. S. Thaxton, C. A. Mirkin, *Science* **2003**, 301, 1884.  
[7] J. Nam, S. Park, C. A. Mirkin, *J. Am. Chem. Soc.* **2002**, 124, 3820.  
[8] J. H. Choy, S. Y. Kwak, J. S. Park, Y. J. Jeong, J. Portier, *J. Am. Chem. Soc.* **1999**, 121, 1399.  
[9] J. H. Choy, S. Y. Kwak, Y. J. Jeong, J. S. Park, *Angew. Chem. Int. Ed.* **2000**, 39, 4041.  
[10] J. Oster, J. Parker, L. A. Brassard, *J. Magn. Magn. Mater.* **2001**, 225, 145.  
[11] S. J. Park, T. A. Taton, C. A. Mirkin, *Science* **2002**, 295, 1503.

[12] X. Zhao, R. Tapeç-Dytioco, K. Wang, W. Tan, *Anal. Chem.* **2003**, 75, 3476.  
[13] C. W. Kwon, A. Poquet, S. Mornet, G. Campet, J. Portier, J. H. Choy, *Electrochem. Commun.* **2002**, 4, 197.  
[14] F. Eckstein, *Oligonucleotides and Analogues: A Practical Approach*, IRL Press, Oxford **1991**.  
[15] R. Massart, *IEEE Trans. Magn.* **1981**, 17, 1247.  
[16] R. Massart, S. Neveu, V. Cauil-Marchal, R. Brossel, J. M. Fruchart, T. Bouchami, J. Roger, A. Bee-Debras, J. N. Pons, M. Carpentier, *French Patent 2 662 539*, **1990**.  
[17] U. Schwertmann, R. M. Cornell, *Iron Oxide in the Laboratory*, Wiley-VCH, Weinheim, Germany **2000**, Ch. 12.

## Membrane Photolithography: Direct Micropatterning and Manipulation of Fluid Phospholipid Membranes in the Aqueous Phase Using Deep-UV Light\*\*

By Chanel K. Yee, Meri L. Amweg, and Atul N. Parikh\*

Surface patterning of physical, chemical, and biological functions using standard photolithographic methods in the dry solid state is leading to new high throughput approaches in materials synthesis,<sup>[1]</sup> sensor microarrays,<sup>[2]</sup> genomics,<sup>[3]</sup> drug screening,<sup>[4]</sup> and proteomics.<sup>[5]</sup> Extending this strategy to fluidic biomembrane functions that require cooperative dynamics and wet environments is desirable in order to understand, emulate, pattern, and exploit many functions of cell membranes for fundamental biophysical research<sup>[6,7]</sup> as well as many biomedical and sensing technologies.<sup>[8,9]</sup> Here, we present a wet photolithographic route for micropatterning fluid phospholipid bilayers<sup>[10]</sup> in which spatially directed illumination with deep-ultraviolet (UV) radiation results in highly localized photodecomposition of the exposed lipids. Unexposed lipids retain their material fluidity and exhibit bio-specific recognitions inhibiting non-specific interactions. Using this method, we can directly engineer stable patterns of hydrophilic voids (with dimensions >2 μm) within a fluid membrane. Furthermore, the voids can be refilled by fusion of secondary lipid vesicles, establishing contiguity with the existing membrane, or creating long-lived, metastably phase-

\* Prof. A. N. Parikh, Dr. C. K. Yee, M. L. Amweg  
Department of Applied Science, University of California  
Davis, CA 95616 (USA)  
E-mail: anparikh@ucdavis.edu

\*\* This work was supported by the University of California, Davis; Los Alamos National Laboratory; Office of Science, BES, U.S. Department of Energy; and the NSF Center for Biophotonics Science & Technology. We thank A. Shreve, S. Simon, N. Jensen, J. Groves, and Y. Yeh for many helpful discussions.

separated states, thereby providing a synthetic means for probing two-dimensional (2D) reaction–diffusion processes, manipulating membrane compositions, and designing functional membrane arrays.

Previously, micropatterning of supported bilayer lipid membranes (sBLMs) has been achieved by two broad classes of method. First, a class of indirect multistep methods has been reported that uses pre-patterned substrates to present chemical and/or electrostatic barriers to membrane formation<sup>[10,20]</sup> or to allow lift-off.<sup>[11]</sup> Patterns of barrier materials are deposited using controlled deposition techniques including photolithography, electron-beam (e-beam) lithography, and micro-contact printing.<sup>[10,12]</sup> Barrier materials have included metals and metal oxides, photoresists, proteins, and photopolymerized lipids,<sup>[13]</sup> but simple mechanical scratches<sup>[14]</sup> have also proved useful.<sup>[13–19]</sup> Second, applications of polymeric

stamps<sup>[20,21]</sup> for direct patterned deposition or removal have also been used. However, several limitations persist. The methods requiring substrate pre-patterning depend on the prior deposition of exogenous materials on the substrate surface and form single, permanent patterns. Methods based on polymer stamps require separate optimization of the contact time and associated contact pressure for different lipid compositions. Moreover, none of these methods can be extended easily to non-planar substrates (e.g., microspheres).

We have developed a simple, light-directed method for direct patterning of sBLMs. The method relies on the spatially directed illumination of sBLMs by deep UV light. The pattern of exposure to light through a mask, or potentially by other spatially addressable means, determines the relief pattern generated within the bilayer. The general procedure that was used is schematically shown in Figure 1. The process begins

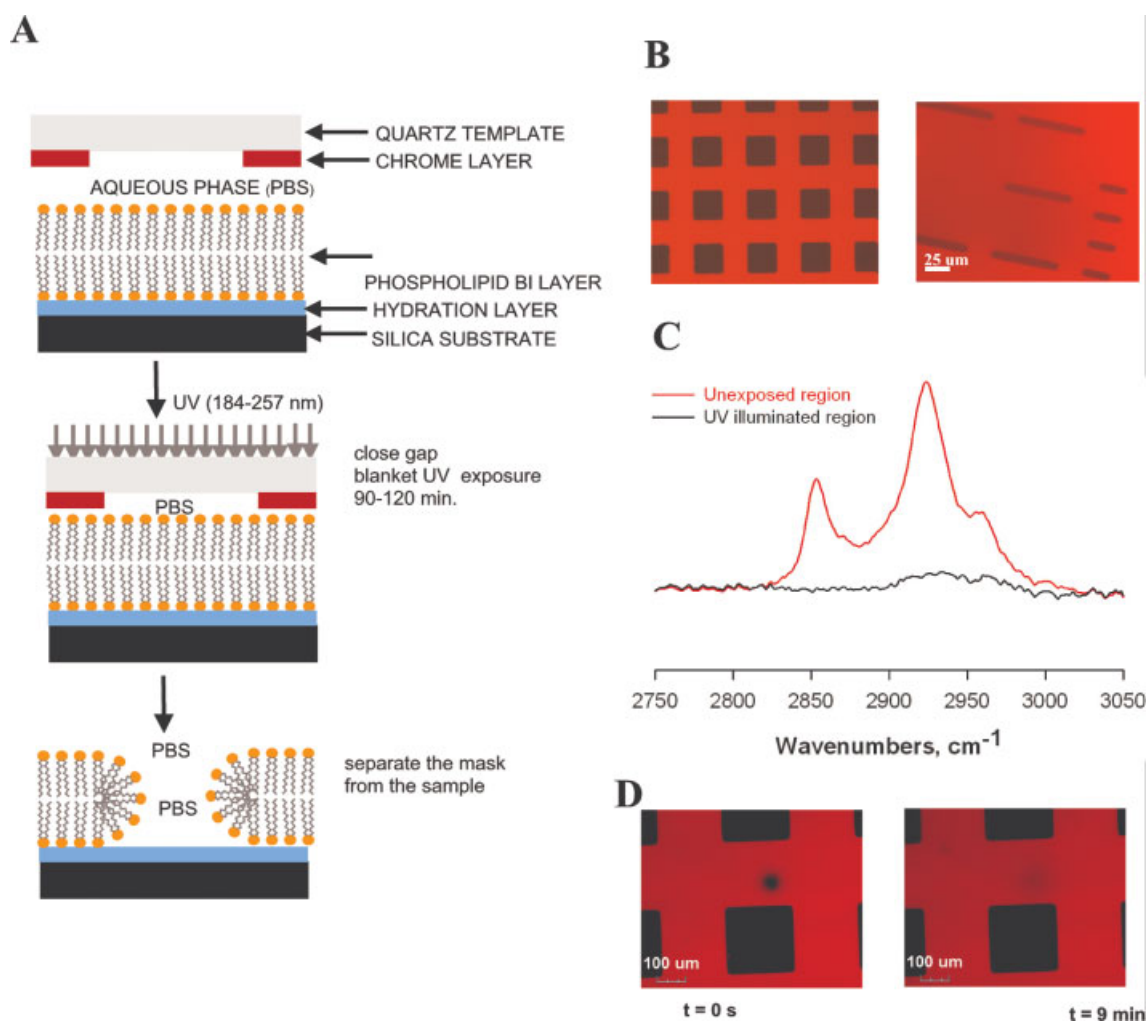


**Figure 1.** Direct patterning of void arrays within bilayer membranes using deep-UV photolithography. A) A schematic diagram of the key process steps. B) A typical epifluorescence image of the void arrays ( $100\ \mu\text{m} \times 100\ \mu\text{m}$ ) obtained using deep UV photolithography within an POPC bilayer membrane supported on a hydrophilic cover glass. C) Spatially resolved ATR-FTIR microscopy spectra in the acyl-chain vibrational mode region ( $2750\text{--}3050\ \text{cm}^{-1}$ ) corresponding to the UV-illuminated and masked bilayer regions revealing the presence and absence of the vibrational mode absorptions due to methylene and methyl groups in lipid molecules. D) Two frames from time-lapse epifluorescence imaging ( $t=0$  and  $t=9\ \text{min}$ ) revealing the fluorescence photobleach recovery for a spot in the vicinity of a void. The rate of recovery confirms the quantitative preservation of probe mobility in the unexposed membrane bilayer.

with the preparation of continuous sBLMs on a hydrophilic surface (e.g., glass or a silicon wafer with a native oxide overlayer). We prepared fluid bilayers of 1-palmitoyl-2-oleoyl-*sn*-glycero-3-phosphocholine (POPC) by adapting previously published methods.<sup>[16]</sup> To enable fluorescence measurements, vesicles were doped with appropriate concentrations of labeled lipids (for details, see the Experimental section). Next, a lithographically produced mask consisting of an array of UV opaque elements (5–1000  $\mu\text{m}$  wide raised 100 nm  $\text{CrO}_2$  features) over a UV transparent quartz was brought in gentle contact with the sBLMs. Deep-UV light in the 184–257 nm range, produced by a low- to medium-pressure Hg lamp housed in a fused quartz envelope, is then directed through the mask at the bilayer samples, which are submerged in phosphate buffered saline (PBS), for ~5–20 min. Upon separation of the mask from the sample under the buffer, high-fidelity patterns of sBLMs comprising intact bilayer regions in the UV-protected areas and lipid-free void regions in the UV-exposed areas were obtained.

Central evidence for the formation of bilayer patterns was provided by the data shown in Figure 1. Optically defined transfer of the mask pattern onto the bilayer is evident in the epifluorescence emission seen in Figure 1B. The data shows a high-contrast fluorescent pattern revealing dark squares, indicating regions devoid of fluorescence emission where UV illumination occurred, separated by bright fluorescent background, corresponding to the protected areas, where the bilayer remains. The patterned sBLMs are stable under aqueous media for several days. A comparison of the attenuated total reflection Fourier transform infrared (ATR-FTIR) microscopy spectra (Fig. 1C) for the dark and bright fluorescent regions reveals the absence of methylene C–H stretching mode absorptions (~2852 and ~2922  $\text{cm}^{-1}$ , respectively<sup>[22]</sup>) in the UV-illuminated (dark) regions, confirming that the dark regions indeed correspond to lipid-free voids. Fluorescence photobleach recovery<sup>[23]</sup> (Fig. 1D) indicated that the lipid bilayer in the UV-protected areas retains its fluidity, characterized by a persistent single translational diffusion coefficient (1–3  $\mu\text{m}^2\text{s}^{-1}$ ) for probe lipids<sup>[23]</sup> with little measurable immobile fraction and no diffusion into the voids.

Repeated patterns with feature definitions as small as 2  $\mu\text{m}$ , visualized using epifluorescence measurements, were found to cover large sample areas, and were only limited by the size of the mask or the substrate. The limiting sizes and densities of patterning were not known, but several factors, including the localization of photooxidation process, fluidity of the bilayer, any expansion at the newly formed lipid front,<sup>[24]</sup> and the diffraction limit of light, are expected to have limiting effects. Typically, the sizes and shapes of the lipid patterns were comparable replicas of the mask pattern but revealed systematic rounding off at the corners. Using this approach, we can create both patterns of voids and isolated membrane islands.

Two well-known processes appear to underscore the mechanism of membrane photolithography. The first is spatially confined photochemical degradation of lipid molecules in the UV-exposed areas. The Hg lamps used in the present study

produce two wavelengths that are absorbed by the material system (lipids and water), 184.9 and 253.7 nm. The shorter wavelength, 184.9 nm, is absorbed by  $\text{O}_2$ , producing two strong oxidants, namely ozone ( $\text{O}_3$ ) and singlet molecular oxygen ( $^1\text{O}_2^*$ ), locally in the vicinity of illuminated regions. The 253.7 nm light is absorbed by the lipids, producing activated molecular species. These species are then readily attacked by  $^1\text{O}_2^*$  and  $\text{O}_3$  to form soluble compounds such as  $\text{CO}_2$ ,  $\text{H}_2\text{O}$ ,  $\text{N}_2$ , etc. which dissolve in the aqueous phase. This process has long been used in waste-water treatment,<sup>[25]</sup> cleaning of semiconductor surfaces,<sup>[26]</sup> and patterning of molecular monolayers.<sup>[27]</sup> Recently Holden and Cremer<sup>[28]</sup> exploited spatially defined production of singlet oxygen during dye photobleaching to pattern dye-labeled molecules and proteins at surfaces. In the present case, the high spatial localization further suggests that the lateral diffusion of individual lipids within the fluid bilayer must be interrupted at an early stage during the photochemical process. Any partially oxidized species that may have diffused within the protected membrane appear not to alter its properties. The second process involves the self-confinement of the unexposed fluid bilayers. The laterally selective removal of lipid molecules leads to the creation of an energetically unfavorable interface, exposing hydrophobic lipid chains to the aqueous medium at the boundary (Fig. 1A). It appears reasonable that the borders, following any edge expansion, shield the hydrophobic chains from the aqueous ambient through reorganization of the lipids during spreading<sup>[24]</sup> into hemi-micelles (Fig. 1A), as observed at the diffusive lipid front.

A useful feature of our approach is that the void pattern within the sBLMs can be refilled by subsequent exposure to “secondary” phospholipid vesicles. When the same lipids are used as secondary vesicles, the membrane patterns can be gradually erased, providing insight into mechanisms of vesicle fusion and spreading. On the other hand, the addition of different lipid types provides a means to manipulate bilayer composition (e.g., spatially controlled insertion, dilution, and localization of desired lipids), study lipid–lipid interdiffusion in 2D bilayer environments, and design long-lived, non-equilibrium mixed lipid phases. In one experiment, we exposed the patterned sBLMs to vesicles of same lipids (with no fluorescent probe-labeled lipids). The lipid was POPC and the initial patterned bilayer was doped with 1 mol-% Texas Red 1,2-dihexadecanoyl-*sn*-glycero-3-phosphoethanolamine triethylammonium salt (TR-DHPE). The time-lapse images in Figure 2B reveal that several minutes after the incubation, the initial non-fluorescent voids acquired fluorescence from the background. An analysis of the time-lapse images reveal gradual pattern transformations, consistent with random Brownian motion of the labeled lipids, ultimately eliminating the fluorescence pattern. The kinetic pattern erasure curves were comparable to the fluorescence recovery curves (see above). These observations indicate that the incoming secondary vesicles must target voids in the bilayer pattern forming non-fluorescent bilayer and become contiguous with the existing fluorescent bilayer through the bilayer–bilayer fusion,

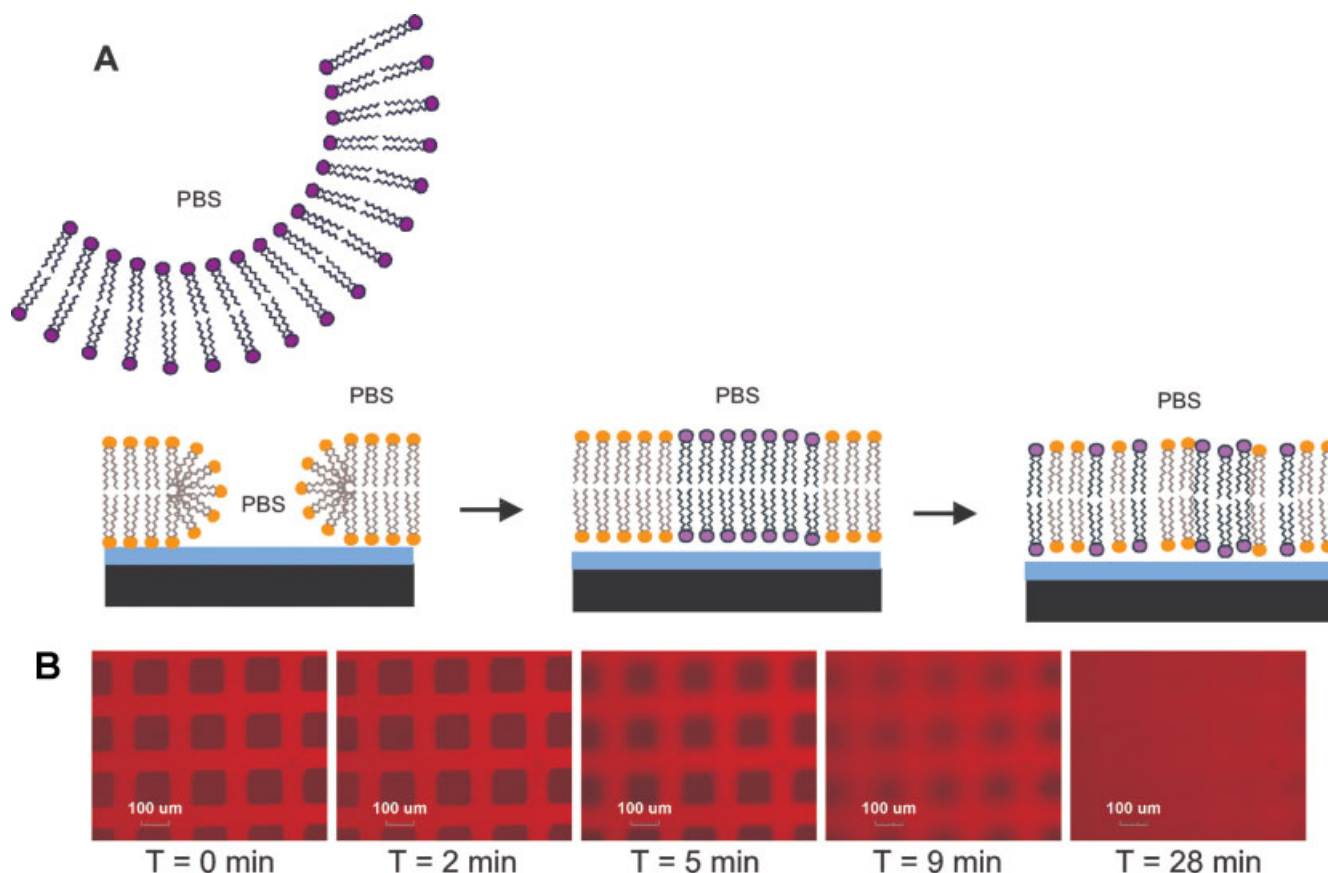


**Figure 2.** Accessibility of void patterns for secondary backfilling. A) A cartoon representation of the process. B) Time-lapse epifluorescence images at arbitrary intervals upon secondary incubation revealing the kinetics of the pattern erasure process. The primary pattern was obtained by membrane photolithography of a TR-DHPE doped POPC bilayer and the secondary backfilling used pure POPC vesicles.

leading to a rate-determining thermal diffusion step (Fig. 2A).

In another experiment, with secondary vesicles containing a lipid mixture believed to represent typical composition of lipid rafts<sup>[29]</sup> (e.g., 37 % POPC, 30 % cholesterol, 28 % sphingomyelin, 2 % GM1 [ganglioside (brain, ovine-ammonium salt)], and 3 % NBD-PE [1-oleoyl-2-[6-[(7-nitro-2-1,3-benzoxadiazol-4-yl)amino]hexanoyl]-*sn*-glycero-3-phosphoethanolamine]), no diffusion of labeled species (NBD-PE or TR-DHPE) across the patterned features occurred for several days. This observation suggests the possibility that raft-like domains (and their aggregates) can be engineered at pre-defined locations within a fluid sBLM background.

Another useful feature of the membrane lithography and backfilling is the provision of well-defined arrays of reaction compartments within the membrane. To illustrate this, we introduced a secondary lipid-mixture containing 1,2-dimyristoyl-*sn*-glycero-3-phosphocholine (DMPC) lipids doped with 1 % *N*-(biotinoyl)-1,2-dihexadecanoyl-*sn*-glycero-3-phosphoethanolamine, triethyl ammonium salt (biotin-DHPE) into the void patterns created in POPC bilayer. By immediately exposing the fresh, unequilibrated mixed lipid surface to

fluorescein labeled streptavidin (FITC-streptavidin), we created patches of 2D streptavidin crystals<sup>[30]</sup> (Fig. 3). Streptavidin patches can be further functionalized using biotinylated species.

In summary, a wet membrane photolithography approach involving spatially directed photodegradation of bilayer lipids using patterned deep-UV illumination is a simple, inexpensive procedure that enables creation of optically defined patterns of fluid bilayers submerged in the aqueous phase. It extends into the aqueous phase popular methods of light-directed syntheses for designing peptides or DNA sequences on planar supports in the dry state.<sup>[3]</sup> The void “barriers” separating the lipid bilayers in this technique are accessible for secondary intercalation by distinct lipids whose approach to equilibrium can be monitored, and the physical basis of membrane heterogeneity can be studied. Moreover, spatially directed insertion of stable functional membrane microenvironments and protein-binding sites is possible. In conjunction with multiple patterning and backfilling cycles, new constructs can be envisaged for high throughput proteomics, membrane-protein arrays, biosensors, and spatially directed, aqueous-phase materials synthesis.

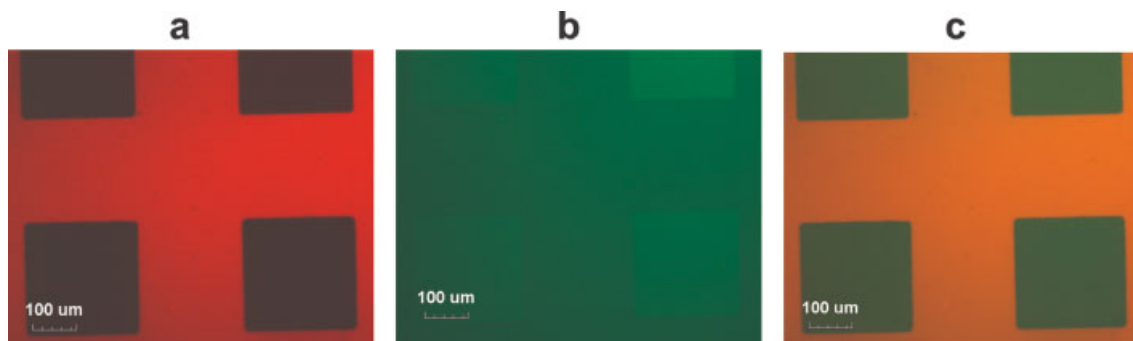


**Figure 3.** Streptavidin arrays. False-color epifluorescence images in a) red, b) green, and c) two-color channels for a FITC-streptavidin arrays within a Texas-Red labeled fluid POPC bilayer.

### Experimental

1-Palmitoyl-2-oleoyl-*sn*-glycero-3-phosphocholine (POPC) and 1,2-dimyristoyl-*sn*-glycero-3-phosphocholine (DMPC) were obtained from Avanti Polar Lipids (Alabaster, AL). Texas Red 1,2-dihexadecanoyl-*sn*-glycero-3-phosphoethanolamine triethylammonium salt (TR-DHPE), *N*-(biotinoyl)-1,2-dihexadecanoyl-*sn*-glycero-3-phosphoethanolamine, triethyl ammonium salt (biotin-DHPE), and fluorescein-labeled streptavidin (FITC-streptavidin) were obtained from Molecular Probes (Eugene, OR). Cholesterol (CH) and sphingomyelin were purchased from Sigma Aldrich (Milwaukee, WI).

Supported phospholipid bilayers were formed using a previously reported vesicle fusion and rupture method [31]. Briefly, small unilamellar vesicles (SUVs) were prepared using vesicle extrusion methods. Typically, a desired amount of lipid or lipid mixtures suspended in chloroform were mixed in a glass vial. The solvent was then evaporated under a stream of nitrogen and subsequently evacuated for at least 1 h in vacuum. The dried lipid mixture was then suspended in Millipore water (18.2 M $\Omega$  cm<sup>-1</sup> resistivity) and kept at 4 °C overnight. The hydrated aqueous solution was then sonicated and passed through an Avanti Mini-Extruder (Avanti, Alabaster, AL) using 0.1  $\mu$ m polycarbonate membrane filters (Avanti, Alabaster, AL) 21 times at the desired temperature. The extruded SUV solution was then diluted with PBS (spreading solution) to 1:1 (v/v). The resulted SUV solutions were stored at 4 °C until use.

Silicon and Corning cover glass substrates prepared for bilayer depositions by immersion in a freshly prepared 4:1 (v/v) mixture of sulfuric acid and hydrogen peroxide maintained at  $\sim$ 90 °C for a period of 5–10 min (caution: this mixture reacts violently with organic materials and must be handled with extreme care). The substrates were then rinsed with copious amounts of Millipore water. Bilayer samples were prepared by placing a clean substrate surface over an  $\sim$ 80  $\mu$ L SUV drop placed at the bottom of a crystallization well. The sample was allowed to incubate for approximately 5 min to ensure equilibrium coverage. The well was then filled with water, then transferred to a large reservoir of water, and the cover slips shaken gently to remove excess vesicles. The sBLM samples prepared in this way were then stored in water or PBS buffer for further use in UV lithography and characterization.

Spatially directed deep UV illumination of supported bilayers was achieved using a physical mask and a deep-UV grid lamp. The masks displaying patterns of chrome over quartz were obtained from Photo-science, Inc (Torrance, CA) and UV radiation was produced using a medium-pressure Hg-discharge grid lamp (10–20 mW cm<sup>-2</sup>, UVP, Inc., Upland, CA) in a quartz envelope, and maintained in a closed chamber. While submerged in buffer, the mask was gently lowered onto the bilayer samples placed in a crystallization dish filled with PBS. The sample system was then carefully placed in an UV/ozone-generating environment so that the cover slips were about 0.2–5 mm away from the light source. The exposure period was approximately

5–20 min. Following the exposure, the samples were immersed in a large water bath, the mask was separated from the substrate surface, and the samples were stored in buffer (or water) for further characterization. Samples were subsequently characterized using epifluorescence microscopies, including imaging and microscopy-based fluorescence photobleach recovery and attenuated total reflection Fourier transform infrared (ATR-FTIR) spectroscopy in a microscope mode (Bruker Optics, Germany).

Received: November 19, 2003  
Final version: February 4, 2004  
Published online: June 29, 2004

- [1] X. D. Xiang, X. D. Sun, G. Briceno, Y. L. Lou, K. A. Wang, H. Y. Chang, W. G. Wallacefreedman, S. W. Chen, P. G. Schultz, *Science* **1995**, 268, 1738.
- [2] H. Bayley, P. S. Cremer, *Nature* **2001**, 413, 226.
- [3] S. P. A. Fodor, J. L. Read, M. C. Pirrang, L. Stryer, A. T. Lu, D. Solas, *Science* **1991**, 251, 767.
- [4] G. A. Michaud, M. Snyder, *BioTechniques* **2002**, 33, 1308
- [5] A. Pandey, M. Mann, *Nature* **2000**, 405, 837
- [6] E. Sackmann, *Science* **1996**, 271, 43.
- [7] S. G. Boxer, *Curr. Opin. Chem. Biol.* **1997**, 387, 580.
- [9] Y. Fang, A. G. Frutos, J. Lahiri, *J. Am. Chem. Soc.* **2002**, 124, 2394.
- [10] J. T. Groves, S. G. Boxer, *Acc. Chem. Res.* **2002**, 35, 149.
- [11] R. N. Orth, M. Wu, D. A. Holowka, H. G. Craighead, B. A. Baird, *Langmuir* **2003**, 19, 1599.
- [12] P. S. Cremer, T. L. Yang, *J. Am. Chem. Soc.* **1999**, 121, 8130.
- [13] K. Morigaki, T. Baumgart, A. Offenhausser, W. Knoll, *Angew. Chem. Int. Ed.* **2001**, 40, 172.
- [14] J. T. Groves, N. Ulman, S. G. Boxer, *Science* **1997**, 275, 651.
- [15] J. Nissen, K. Jacobs, J. O. Radler, *Phys. Rev. Lett.* **2001**, 86, 1904.
- [16] J. T. Groves, S. G. Boxer, *Biophys. J.* **1995**, 69, 1972.
- [17] L. A. Kung, L. Kam, J. S. Hovis, S. G. Boxer, *Langmuir* **2000**, 16, 6773.
- [18] K. Morigaki, T. Baumgart, U. Jonas, A. Offenhausser, W. Knoll, *Langmuir* **2002**, 18, 4082.
- [19] L. A. Kung, J. T. Groves, N. Ulman, S. G. Boxer, *Adv. Mater.* **2000**, 12, 731.
- [20] J. S. Hovis, S. G. Boxer, *Langmuir* **2001**, 17, 894.
- [21] J. S. Hovis, S. G. Boxer, *Langmuir* **2001**, 17, 3400.
- [22] L. K. Tamm, S. A. Tatulian, *Q. Rev. Biophys.* **1997**, 30, 365.
- [23] D. A. Axelrod, D. E. Koppel, J. Schlessinger, E. Elson, W. W. Webb, *Biophys. J.* **1976**, 16, 1055.
- [24] J. Nissen, S. Gritsch, G. Wiegand, J. O. Radler, *Eur. Phys. J. B* **1999**, 10, 335.
- [25] O. LeGrini, E. Oliveros, A. M. Braun, *Chem. Rev.* **1993**, 93, 671.

- [26] J. R. Vig, *J. Vac. Sci. Technol. A* **1995**, *3*, 1027.  
[27] C. S. Dulcey, J. H. Georger, V. Krauthamer, D. A. Stenger, T. L. Fare, J. M. Calvert, *Science* **1991**, *252*, 551.  
[28] M. A. Holden, P. S. Cremer, *J. Am. Chem. Soc.* **2003**, *125*, 8074.  
[29] K. Simons, E. Ikonen, *Science* **2000**, *290*, 1721.  
[30] R. Blackenburg, P. Meller, H. Ringsdorf, C. Saless, *Biochemistry* **1989**, *28*, 8214.  
[31] L. D. Mayer, M. J. Hope, P. R. Cullis, *Biochim. Biophys. Acta* **1986**, *858*, 161.

## (Ti,Sn)O<sub>2</sub> Solid Solution Self-Aligned into “Sandwich” Array on Grafted Modification Collagen Matrix\*\*

By Yong Cao, Yu Ming Zhou,\* Yun Shan, Huang Xian Ju,\* Xue Jia Xue, and Zong Han Wu

Monolayer and multilayer films with morphology-controllable structures are promising for applications in building novel sensor devices, light-emitting diodes, biomedical coatings, and in creating organically based nonlinear optical materials.<sup>[1]</sup> Various approaches, including spin-coating, the Langmuir–Blodgett technique, electrostatic adsorption of oppositely charged polyelectrolytes, and covalent attachment of polymers using conventional coupling chemistry, have been used to produce complex nanostructures and have been developed for preparing different hybrids with diversified morphologies.<sup>[2]</sup> The general utility of these methods has been further extended by incorporating nanocrystals into polymer matrices.<sup>[3]</sup> The versatility and complexity of these polymeric composites provide new opportunities in the semiconductor, photovoltaic, and molecular electronic fields.<sup>[4]</sup> However, it is still important to study thin-film preparation in various media and with a variety of modification agents.<sup>[5]</sup>

Incorporating metal nanocrystals in biological systems is a widespread, yet incompletely understood, procedure, involving complex interactions at the biomacromolecule–metal nucleus interface.<sup>[6]</sup> Studying this process may help us to understand and control the formation of metal nanocrystals in a generalized peptide–amphiphile chain system. Two major approaches have been developed to organize metal nanoparticles into polymer substrates.<sup>[7–12]</sup> The first method involves the self-coding of nanoparticle building blocks that can be coupled via interparticle connectors with specific recognition properties based on, for example, DNA duplex formation,<sup>[7]</sup> antibody–antigen specificity,<sup>[8]</sup> streptavidin–biotin coupling,<sup>[9]</sup> electrostatic matching,<sup>[10]</sup> or shape-directed hydrophobic forces.<sup>[11]</sup> Another method, the template-directed approach,<sup>[12]</sup> utilizes porous solid substrates or discrete liquid droplets as patterned or shaped interfaces for the assembly of preformed nanoparticles. In this process capillary, drying, and swelling forces, or other chemical interactions, are used to implant, position, and immobilize nanoparticles irreversibly within the template or around the surface of individual latex beads pre-coated with a layer-by-layer shell of oppositely charged polyelectrolyte macromolecules. However, to the best of our knowledge, there has been no previous example of incorporating bimetal solid solutions into a biological system in order to form a well-defined morphology without using any template or specific recognition interparticle connectors.

Herein, we present a versatile procedure, based on the self-assembly process, for preparing a large-area nanoscale “sandwich” layer array of tailored composition, with a controllable crystalline phase and defined morphology. The idea for creating this composite film was stimulated by Yang and Rubner,<sup>[13]</sup> who developed a novel assembly method by using hydrogen-bonding interactions to fabricate a polyelectrolyte multilayer film. Differing from their work, we employed a protein with a unique tertiary structure, collagen—whose stalks consist of right-handed supercoils of three left-handed polyproline II-type helices with major sequences of (Gly–Pro–Hyp)<sub>n</sub><sup>[14,15]</sup>—to design and synthesize an ordered biological scaffold, and to control the growth of various metals in an exact arrangement, with high reproducibility and accuracy, by using two uniform interactions of both hydrogen bonding and covalent bonding between the biomatrix and the nanocrystals.<sup>[16]</sup> This strategy combines organic modification with metal-assisted stabilization of collagenous triple helices in order to achieve an ordered assembly architecture, which is distinctly different from the previous methodologies, such as those used by Koide and co-workers<sup>[14,17]</sup> and Babu and Ganesh, to modify collagen.<sup>[15]</sup> A model of multiple spatial interactions (covalent bonding and hydrogen bonding) existing in this system is shown in Scheme 1. These two tethering forces allow a certain degree of mobility and an enhanced long-term periodicity. In particular, this synthetic procedure was carried out without heating or adding any organic surfactant or direction-guiding agent. The film was formed in an aqueous system at a relatively low temperature, in a simple and rapid process. Unlike ordinary Langmuir–Blodgett (LB) films, the prepara-

[\*] Prof. H. X. Ju, Dr. Y. Cao  
Laboratory of Analytical Chemistry for Life Science  
Department of Chemistry, Nanjing University  
Nanjing, 210093 (P.R. China)  
E-mail: hxju@nju.edu.cn

Prof. Y. M. Zhou, Y. Shan, X. J. Xue  
Department of Chemistry and Chemical Engineering  
University of Southeast  
Nanjing, 210096 (P.R. China)  
E-mail: Ymzhou@jlonline.com

Prof. Z. H. Wu  
Department of Physics  
University of Southeast  
Nanjing, 210096 (P.R. China)

[\*\*] We gratefully acknowledge the National Natural Science Foundation of China (No. 50377005, 50177005, 20325518), the Advanced Technology and Natural Science Foundation supplied by the Science and Technology Department of Jiangsu Province (No. BG 2001034, BK 2003064), and the Science Foundation of Southeast University (No. 9207041139) for their financial support of this research. Supporting information is available online from WileyInterscience or from the authors.